PHYSICAL REVIEW B VOLUME 24, NUMBER 10 15 NOVEMBER 1981

Relationship between surface-plasmon radiation and enhanced adsorbate Raman scattering

G. L. Eesley
Physics Department, General Motors Research Laboratories, Warren, Michigan 48090-9055
(Received 11 June 1981)

We present the first experimental results which verify a quadratic relationship between the enhanced Raman scattering from Ag surfaces and roughness coupled surface-plasmon radiation. Additionally we show that the enhanced Raman signal results from an interaction with a continuum of excitations in the visible region of the spectrum and not from an interaction with the peak surface-plasmon excitation.

INTRODUCTION

The enhancement in Raman scattering from molecules adsorbed on specially prepared silver (Ag) surfaces has attracted much experimental attention and theoretical controversy in recent years.[1] It has now been established that at least one universal requirement for observing large enhancements ($>10^3$) is some degree of submicroscopic surface roughness. This observation has resulted in several theoretical proposals which relate the enhanced adsorbate Raman scattering[2] (EARS) to the roughness assisted radiative excitation of surface plasmons,[3] polaritons,[4] collective electron resonances,[5–7] dipolar plasmons,[8] etc.

On a smooth surface, the surface plasmons have a wave vector $\vec{k}_p$ always greater than that of photons ($k=\omega/c$) and thus radiative coupling is very weak. However, on a rough surface the ground state of a plasmon is no longer a single harmonic wave with wave vector $\vec{k}_p$. Through scattering off of the periodic potential $V(\vec{K})$ of the rough surface, the plasmons attain components $\vec{k}_p+\vec{K}$ and shifts in resonant frequency $\omega(\vec{k}_p)\rightarrow\omega(\vec{k}_p+\vec{K})$ occur if the scattering is inelastic.[9] Analogous to this situation is the dramatic shift in plasmon-induced optical resonances associated with colloidal suspensions of metallic clusters. These shifted resonances result from the boundary conditions imposed by the shape, ambient medium, and the submicroscopic dimensions of the individual clusters.[6] A graphic demonstration of this effect is the rather strong visible absorption resonance observed in colloidal suspensions of Ag clusters, even though the infinite-plane surface-plasmon resonance for Ag is in the ultraviolet.[10–13] Similar behavior is observed in Cu and Au suspensions, and this has been interpreted as evidence for a surface-plasmon (SP) model of the EARS which is observed from Ag, Cu, and Au supported molecules.

Various models account for EARS by invoking surface-plasmon excitation and by calculating the SP local field experienced by adsorbed molecules. It is shown that SP excitation by incident light waves can produce a local field much larger than the incident light field.[3] Thus, in a very straightforward manner the adsorbed molecules are found to Raman scatter more efficiently. In most cases, the coupling of the SP to the adsorbed molecules has been treated on a purely electromagnetic basis and this has led to predictions of a long-range enhancement extending ~ 10 nm beyond the surface. In an attempt to reconcile observations of both a short-range enhancement[14–16] and the long-range enhancement,[16–18] Jha *et al.*[19,20] have also accounted for scattering of the SP excitations from the vibrating molecular potential.

A review of the details of the various SP theories is beyond the scope of the present experimental work. We only remark that in most cases the EARS is described by resonant radiative coupling with two SP excitations: (1) the excitation at the incident light frequency ω_L and (2) the excitation occurring at the Raman-scattered light frequency ω_S. As a result, we may expect the EARS signal to depend quadratically on the SP radiative coupling. Recent experimental work has shown a correspondence between the Raman enhancement and the light absorption profile versus Ag film roughness.[21] In addition Chen and Burstein[7] have explicitly proposed that the EARS signal should scale quadratically with the SP light absorption

and they have alluded to results which approximately verify this. Nevertheless, absorption measurements do not unambiguously verify the SP models. As pointed out by Weber and Ford,[22] the absorption of incident light may be the result of a strong coupling between the image enhanced near field of the molecule and nonradiative surface waves. In addition, the roughness may also facilitate electron-hole pair generation which may or may not be considered a dissipative process. Thus, the relationship between roughness coupled SP *emission* and the EARS signal can provide crucial evidence for the EARS—surface-plasmon interaction. After all, the EARS phenomenon is observed as an increased *emission* of Stokes shifted photons.

In the following we present the first quantitative results which verify a quadratic relationship between the EARS signal and the roughness coupled SP radiation. These results can be explained by a model which includes both roughness assisted SP scattering and SP radiative coupling. However, we show that the EARS signal does not rely on a singular resonance with the peak SP excitation, but rather on an interaction with a continuum of optical excitations in the visible region of the spectrum. The dominant roughness coupled SP optical resonance shifts to slightly lower energies than the smooth surface resonance, but still remains distant from the laser and Stokes frequencies.

We also use a novel method to determine that a 35-nm roughness periodicity results in our maximum observed enhancement. This determination is made *in situ*, independent of scanning electron micrographs[14,17,21] or the use of film thickness measurements.[23] A discussion of our data in terms of alternative enhancement models is given as well.

EXPERIMENTAL

The experiments were performed in a conventional ultrahigh vacuum (UHV) system with a base operating pressure of 2×10^{-8} Pa. The UHV system is equipped for Auger electron spectroscopy (AES), low-energy electron diffraction (LEED), mass spectroscopy, and Raman spectroscopy (for details see Ref. 24). In addition to this equipment, we have also mounted an electron gun which points at the Ag target when it is optically aligned for Raman investigations. By firing a 1 keV, 0.83-μA beam of electrons at an $\sim80°$ angle of incidence, we can excite and monitor surface-plasmon fluorescence (details in the next section) from the same point on the Ag which is probed by the Raman technique. Raman and SP light emission are collected normal to the Ag surface by an $f1$ optical system and analyzed by a double monochrometer.

The Ag used in this work was a ~2-cm^2, 2-mm thick slice taken from a single-crystal (110) rod of 99.999% purity. The single-crystal slice was polished with Linde 0.05-μm powder, ultrasonically cleaned in acetone and etched for ~1 sec in a 1:1 solution of hydrogen peroxide (50% strength) and ammonium hydroxide. The rapid etch is quenched in isopropyl alcohol. The resulting Ag surface possesses a mirror finish, with the etch removing many of the polishing scratches. Following this procedure, the Ag is mounted on a manipulator and placed immediately in the UHV chamber. Several annealing cycles to $+150$ °C and subsequent 500-V argon-ion sputters (1.3×10^{-3} Pa) removed the C, N, S, and Cl contamination detected by AES. LEED verified that the resulting Ag surface was indeed single crystal (110). This nominally "smooth" surface was used for the initial SP emission and Raman measurements to be described later.

A roughened surface structure was produced electrochemically, and this required removal of the Ag from the UHV chamber. A radially varying roughness profile was achieved by positioning the Ag slice horizontally below a Pt mesh counter electrode (wrapped around a cotton swab, ~2 mm above the Ag surface). A 0.1 molar KCl solution was dropped onto the Pt mesh-cotton structure and this formed an electrolytic bridge to the Ag surface. The resulting solution bridge covered three-fourths of the single-crystal surface, with the outer-surface edges remaining exposed to air. After a single oxidation-reduction cycle and rinsing with distilled water and methanol, the Ag was reinserted into the chamber. A 180-min argon-ion sputter (1000 V, 6×10^{-3} Pa) removed residual traces of K and Cl as detected by AES.

The appearance of this processed Ag surface was hazy white in an annular ring (outside radius—inside radius ~0.5 cm) surrounding a central area which was smooth and polycrystalline. At the extreme outside radius of the ring, there was a transition back to nominally single-crystal Ag. In the subsequent experiments, varying degrees of roughness were sampled by the focused laser and electron beams by translating the Ag in a radial direction.

SURFACE-PLASMON SPECTRA

Several mechanisms can produce radiation as a result of energetic electrons incident on a metal

surface. When the electron enters the surface, transition radiation is produced by the collapsing dipolar field, and bremsstrahlung is produced by electron scattering in the metal.[25] These processes produce a spectrum composed of a peak or shoulder at the volume-plasmon frequency of the metal, with a continuum of emission extending to lower frequencies. The incident electrons can also excite surface-plasmon (SP) waves which will decay via roughness coupled radiation.[26,27] Generation of the SP radiation by low-energy electrons was recently demonstrated by Chung *et al.*[28] An adequate theoretical description of the generation of roughness coupled SP radiation was proposed by Kretschmann *et al.*[29] and the results will be briefly summarized here.

The metal surface roughness is usually modeled by an autocorrelation function parametrized by the mean-square roughness amplitude and the average roughness wavelength along the surface. If the Fourier transform of the surface roughness correlation function [wave-vector spectral density $=g(K)$] can be represented by the sum of a broadened low-wave vector part, $g_l(K)$, and a dominant high-wave vector part, $g_h(K)$, then

$$\langle s^2\rangle g(K)=\langle s_l^2\rangle g_l(K) + \frac{\langle s_h^2\rangle}{2\pi}\left[K_h\left[\frac{\omega}{c}\right]^2\right]^{-1}\delta(K-K_h)\,, \quad (1)$$

where $g_h(K)$ is represented by a delta function at wave vector $K_h >> 1$, and $\langle s^2\rangle=\langle s_l^2\rangle+\langle s_h^2\rangle$ represents the mean-square roughness height. Kretschmann *et al.*[29] have shown that the differential scattering cross section for electron-induced, roughness coupled SP radiation at resonance scales as

$$\frac{\partial^2}{\partial\omega\partial\Omega}\sigma_h \propto \langle s_h^2\rangle\left[\frac{\omega}{c}\right]^2\beta^2K_h^2/\,|\,1+\beta^2K_h^2\,|^2\,, \quad (2)$$

where $\beta=v/c$ is the normalized electron velocity. The unique feature of Eq. (2) is that we may measure the SP emission-peak height as a function of electron energy, and by fitting the normalized data to Eq. (2) we may extract a value for $K_h=\lambda_p/\lambda_h$, where λ_p is the peak SP emission wavelength and λ_h is the dominant roughness wavelength. We will return to this point later.

The SP spectra which result from 1-keV electrons incident on our Ag sample are shown in Figs. 1(a)—1(e), where the emission frequency is in units of cm^{-1} ($\omega/2\pi c$). Spectrum (a) corresponds

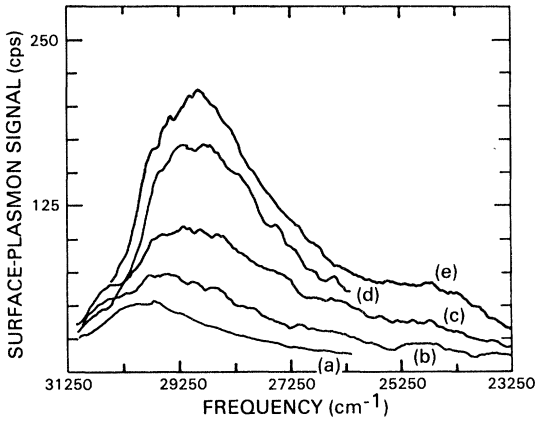

FIG. 1. Surface-plasmon emission spectra from single-crystal Ag(110) in (a), and progressively rougher Ag in (b)—(e).

to the initially smooth single-crystal surface, and spectra (b)—(e) correspond to successively rougher positions on the Ag surface. The SP emission was measured every 25 cm^{-1} in the 31250—23250 cm^{-1} region and the spectra in Fig. 1 result from a 15-point smoothing routine. The spectrometer resolution for all the SP data collection was ~30 cm^{-1}, and a 10-sec count time per data point was used.

A general feature of all the spectra in Fig. 1 is the volume-plasmon emission shoulder at 30250 cm^{-1} (330.6 nm), which is easily visible in the single-crystal spectrum of Fig. 1(a). As the roughness of the surface increases, we find that the SP emission peak at 29725 cm^{-1} (336.4 nm) on the smooth surface shifts to lower frequencies and increases in amplitude. The increased peak amplitude would be expected for an increased roughness amplitude $\langle s\rangle$, but the shift to lower frequency may indicate that a different roughness wave vector is dominating each of the spectra in Fig. 1.

Beyond 23250 cm^{-1} (430.1 nm), all SP spectra are comprised of a featureless continuum which extends to frequencies below 16250 cm^{-1} (615.4 nm). We have found that to within experimental error, the amplitude of the continuum emission is linearly related to the amplitude of the corresponding SP peak emission. Thus we will use the more accurate SP peak emission count rates for further analysis.

Since the ultimate goal is to relate the SP radiation to the Raman scattering enhancement, some attempt must be made to correct the peak signals of Figs. 1(b)—1(e) for any background transition radiation and/or bulk-plasmon radiation. To do so, we use the spectrum of Fig. 1(a) which corresponds

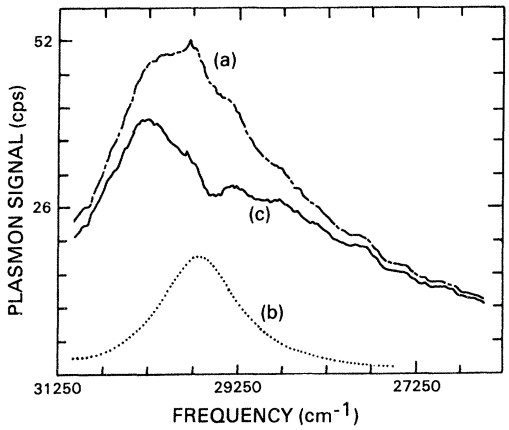

FIG. 2. Calculation of the bulk plasmon + transition radiation contribution to the (a) smooth Ag(110) spectrum. The assumed SP resonance of Lorentzian line shape (550 cm^{-1} half width at half maximum, 18-cps height) at 29 675 cm^{-1} (b) is subtracted from (a) resulting in spectrum (c).

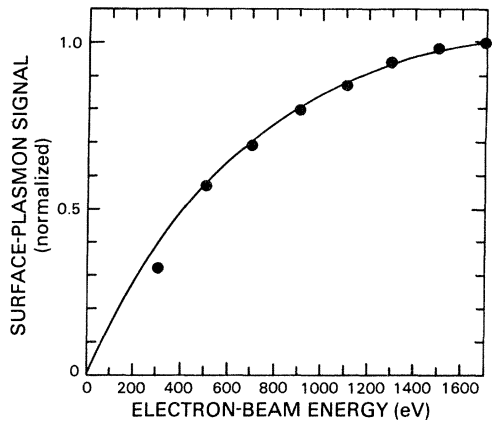

FIG. 3. Normalized variation of the SP peak height in Fig. 1(e) with incident electron energy. The solid curve is a single parameter fit ($K_h = 10$ of Eq. (2) to the data (●).

to the single-crystal Ag(110) surface. We note that although a sharp LEED pattern was visible from this surface, it was not ideally "smooth," otherwise the SP emission peak at 29 725 cm^{-1} would not be visible in Fig. 1(a). To correct for this small amount of roughness coupled radiation in Fig. 1(a), we have subtracted SP emission by assuming a Lorentzian line shape with a half width of 550 cm^{-1}, a peak height of 18 counts per second (cps) and a peak location of 29675 cm^{-1} (336.9 nm). The resulting spectrum is shown in Fig. 2, where the dotted line represents the assumed SP peak, the dashed line the real data, and the solid line the net bulk-plasmon and transition radiation spectrum. This background spectrum will be subtracted from the roughness coupled spectra in Figs. 1(b)—1(e) and the resulting peak SP count rates will be correlated with the Raman data in the next section.

Finally, we may estimate the roughness periodicity corresponding to Fig. 1(e) by fitting Eq. (2) to the variation of the SP peak height (at 28900 cm^{-1}) with incident electron energy. Figure 3 displays a fit (solid line) of Eq. (2) normalized and plotted versus the electron beam energy. The dots correspond to the SP peak height normalized to the value measured at 1700 eV. The only free parameter for the curve fit is K_h, the dominant roughness wave vector. The fit is remarkably good and indicates a dominant roughness wavelength of $\lambda_h = 34.6$ nm ($K_h = 10$). This value of λ_h is comparable to the optimum (with regard to EARS) values found by scanning electron micrographs[14,17,21] and film thickness measurements.[23]

CORRELATION WITH RAMAN ENHANCEMENT

In all cases of enhanced adsorbate Raman scattering, it has been observed that a broad continuum background accompanies the adsorbate Raman spectrum. Chen *et al.*[30] have verified that the magnitude of the enhancement is related linearly to the background signal, and this relationship was also observed for the present Ag surface. Thus, any correlation between the Raman background continuum (on a clean substrate) and the SP emission will also represent the correlation between the EARS signal and the SP emission. It is only necessary to measure the Raman background continuum at the same positions on the Ag surface which produced the SP spectra of Fig. 1.

The Raman background measurements were made at a Raman shifted frequency of 960 cm^{-1} (18475 cm^{-1} absolute frequency), using 100 mW of 514.5-nm argon-ion laser emission, a spectrometer resolution of ~6 cm^{-1}, and a 60-sec count time. The results of these measurements are tabulated in Table I, along with the SP peak location and signal level (after correcting for the background transition radiation). The SP continuum emission was calculated from a 20-point average of the emission signal between 19450 and 18450 cm^{-1}. These signal values are less reliable than the SP peak emission measurements, since the scattered electron-gun filament light was 2—3 orders of magnitude larger in the visible region of the spectrum. Even so, it appears that the ratio of the

TABLE I. Surface plasmon and Raman signals.

Fig. 1	SP peak frequency (cm^{-1})	Bulk plasmon + transition radiation (cps)	SP peak emission (cps)[a]	SP continuum (cps)[b]	Raman background (cps)[c]
(a)	29 725	34	18		15
(b)	29 475	27.5	46.4	7	628
(c)	29 175	28.6	81.5	13.8	1886
(d)	28 950	27	144.3	18.4	5410
(e)	28 900	27	185.1	25.3	9779

[a]Bulk plasmon + transition radiation subtracted.
[b]A twenty point average of count rates measured between 19450 and 18450 cm^{-1}.
[c]At 960-cm^{-1} Raman shift; 60-sec count time.

peak SP emission to continuum emission is approximately 7 for all points.

The correlation between the enhanced Raman background signal and the corrected peak SP emission (from Table I) is shown in Fig. 4. Both the Raman background and the SP signals are normalized to their respective maxima and plotted on a log-log scale. A least-squares fit of the data to the equation $I_{EARS}=aI_{SP}^{b}$ yields values $a=1.06$ and $b=1.96$, with a coefficient of determination $r^2=0.99$ ($r^2=1$ implies a perfect fit). Thus we find that the EARS scales quadratically with the roughness coupled SP radiation. We note however, that the slope b of the line in Fig. 4 is sensitive to the amount of bulk-plasmon and transition radiation subtracted from the SP peak signal. Without this correction, a value of $b=2.6$ is obtained.

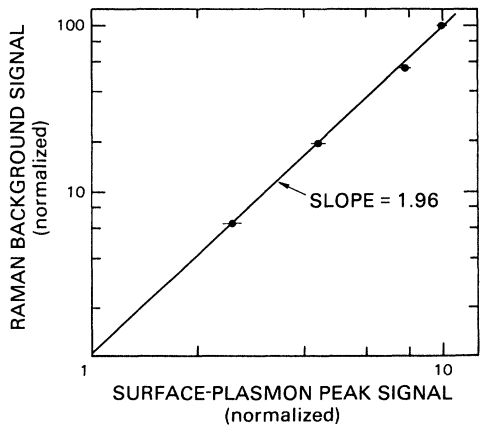

FIG. 4. Normalized log-log plot of the enhanced Raman background signal versus the SP peak signal. Error bars are visible for the SP signal only.

We also point out that there was no observation of EARS from pyridine on the single crystal Ag which produced the SP spectrum of Fig. 1(a), and the corresponding peak SP emission (18 counts/sec) and the EARS background (~ 15 counts/sec) do not correlate with the data in Fig. 4. Recent observations by Udagawa *et al.*[31] of EARS on Ag(111) may indicate another weak (below our detection limit) mechanism is operative on smooth surfaces.

DISCUSSION

The preceding analysis demonstrates that the EARS mechanism can be related in a simple quantitative way to the surface-plasmon emission from roughened Ag surfaces. Rigorously, however, we can only state that the roughness which radiatively couples the SP also results in an enhanced Raman scattering mechanism which is suggestive of a two-plasmon interaction.

To gain some insight into the physical processes responsible for this interaction, we refer to the interaction diagram of Fig. 5. The solid line in Fig. 5 represents the evolution of surface plasmons from intitial state $|i>$ to final state $|f>$. The wiggly diagonal lines represent photon modes with occupation numbers m_L (frequency ω_L) and m_S (frequency ω_S). The intersection of a photon line with the plasmon line represents an interaction vertex which may be mediated by the roughness potential $V(\vec{K})$ of the surface plane ($==x$). In the formalism of Wilems and Ritchie,[27] the rough surface potential can be related to a charge-density fluctuation at the surface resulting from structural irregularities. This potential could also be modified to

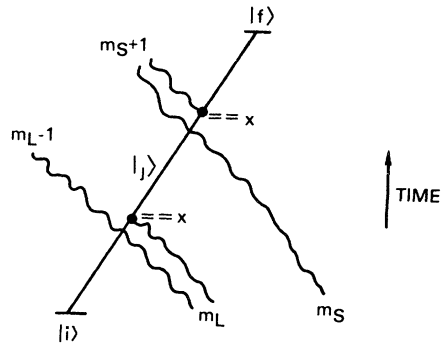

FIG. 5. A time-ordered photon interaction diagram representing the EARS process. A photon mode (ω_L; occupation number m_L, frequency ω_L) excites a surface plasmon (ω_j) from state $|i>$ to $|j>$ via the rough surface potential ($=\!=x$). This excited SP scatters inelastically from the surface potential, radiates (ω_S) into a photon mode (occupation number m_S, frequency ω_S) and relaxes to state $|f>$.

include the density fluctuations resulting from a molecular vibrational potential as proposed by Jha *et al.*[19]

In the time-ordered process shown in Fig. 5, a photon of frequency ω_L excites a SP from initial state $|i>$ to intermediate state $|j>$ through interaction with the rough surface potential. This SP scatters inelastically from the surface potential by radiating a photon at frequency ω_S, and thereby relaxes to final state $|f>$. (The details of the scattering process are not important to our discussion.)

Ritchie[26] has shown that the plasmon-radiation interaction Hamiltonian can be represented by

$$H_{\mathrm{PR}} \propto \int d^2\vec{r}\; V(\vec{r})\hat{A}_P\cdot\hat{A}_R \;, \tag{3}$$

where $\hat{A}_P$ and $\hat{A}_R$ are the plasmon and photon vector potential operators, respectively, and $V(\vec{r})$ is the rough surface potential in real space. If the scale of roughness is small compared to the wavelength of light, then the expectation value of H_{PR} will be proportional to a two-dimensional integral over the surface of the metal

$$\langle H_{\mathrm{PR}}\rangle \propto \int d^2\vec{\rho}\; V(\vec{\rho})e^{i(\vec{k}_j-\vec{k})\cdot\vec{\rho}} = V(\vec{K}) \;, \tag{4}$$

where $\vec{k}_j$ and $\vec{k}$ are the wave vectors of the surface plasmon and photon, respectively. The interaction of Fig. 5 represents to lowest order in $V(\vec{K})$ the process by which Raman shifted photons may be generated, and from Fermi's golden rule we find the transition rate will follow,

$$R(\mathrm{EARS}) \propto \left|\sum_j \frac{\langle H_{\mathrm{PR}}\rangle_L\langle H_{\mathrm{PR}}\rangle_S}{\omega(\vec{k}_L)-\omega(\vec{k}_j)+i\Gamma(\vec{k}_j)}\right|^2$$

$$\propto |V(\vec{K})|^4 \;, \tag{5}$$

where $\omega(\vec{k}_\alpha)$ is the frequency of either a photon (L) or plasmon (j) with wave vector $\vec{k}_\alpha$ and $\Gamma(\vec{k}_j)$ is the plasmon damping rate. The important result here is the dependence of the Raman interaction on $|V(\vec{K})|^4$, where $|V(\vec{K})|^2$ is directly related to the Fourier transform of the autocorrelation function for surface roughness, $g(\vec{K})$. From the work of Ritchie[26] and Kretschmann *et al.*,[29] we find that the rate for electron-excited, roughness coupled SP radiative emission (EESP) scales as $|V(\vec{K})|^2$ and therefore

$$R(\mathrm{EARS}) \propto [R(\mathrm{EESP})]^2 \;, \tag{6}$$

which is precisely the relationship observed in our experiment.

These results appear encouraging from the standpoint of the $V(\vec{K})$ dependence of the matrix elements in Eq. (5), but a comparison of the energy denominator with the SP spectra in Fig. 1 may raise some questions regarding the predictions of resonantly enhanced SP coupling.[3,5,6,8] Can the long continuum tail of the SP emission spectra be considered as a sum of spatially localized plasmon resonances defined by independent clusters of roughened Ag on a smooth supporting substrate (inhomogeneous broadening)? Or is the continuum tail the result of lifetime broadening of the dominant SP peak in the near ultraviolet region of the spectrum (homogeneous broadening)? If the former question were true, then the overall rate of Eq. (5) would be additionally enhanced by the coincidence between photon and plasmon energies, adding credibility to the surface-plasmon interpretation of EARS. However, if the SP emission is solely lifetime broadened, then the large frequency mismatch $\omega(\vec{k}_j)-\omega(\vec{k}_L)$ and large $\Gamma(\vec{k}_j)$ in the denominator of Eq. (5) reduce the credibility of this model for EARS.

It must also be pointed out that the electron-hole pair excitation model for EARS proposed by Burstein *et al.*[32] Billman *et al.*[33] and Otto *et al.*[34] would be analogous to that depicted in Eq. (5). That is, radiative coupling to electron-hole pair excitations via surface roughness might lead to a transition rate scaling as

$$R(\mathrm{EARS}) \propto \left|\sum_j \langle H_{e\text{-ph}}\rangle_L\langle H_{e\text{-ph}}\rangle_S\right|^2 \propto |V(\vec{K})|^4 \;, \tag{7}$$

to lowest order in $V(\vec{K})$, where $H_{e\text{-ph}}$ represents the electron-photon interaction Hamiltonian. The details of this mechanism appear to be less well understood than those of the SP mechanisms, and the amount of supporting evidence is substantially less.

Additionally, one may expect a similar dependence on the surface autocorrelation function for the "lightening rod" mechanism proposed by Gersten.[35] However, this model appears to be sensitive to the exact details of surface geometry and this information is not contained explicitly in the surface autocorrelation function.

CONCLUSIONS

We have investigated the correlation between roughness coupled surface-plasmon radiation and the enhanced adsorbate Raman scattering process. It is found that the EARS signal is related quadratically to the peak SP radiation excited by 1-keV electrons incident on a rough Ag surface. A plausible explanation for this dependence arises from the SP—Raman enhancement models[3,4] which account for a SP—photon coupling at both the laser and Stokes shifted optical frequencies. We have shown that to lowest order, these models depend quadratically on the wave-vector spectral density (i.e., the Fourier transform of the roughness autocorrelation function) of a roughened metal surface. Our results also support the prediction by Chen and Burstein[7] that the EARS mechanism should scale quadratically with the SP absorption of light on rough surfaces.

Predictions by Aravind and Metiu[36] and Weber and Ford[22] that the EARS process depends linearly on the roughness autocorrelation function would appear invalid for the system we have studied. However, these models may become more important on smoother surfaces where very few observations of EARS have been made.[31,37]

More theoretical work regarding the electron-hole pair enhancement model of Otto *et al.*[34] is necessary before any serious attempt is undertaken to distinguish this mechanism from the SP interaction. It is very likely that an important atomic scale roughness accompanies the grosser roughness features dealt with in our study. This could also result in a linear scaling of the EARS signal with the Raman continuum and the quadratic relationship between EARS and the SP peak radiation. A survey of the various EARS spectra in the literature would indicate varied ratios of the EARS signal to the Raman continuum, although each individual would likely find a linear dependence between the EARS signal and continuum for the various degrees of roughness on a particular surface. This may indicate that variations in atomic scale roughness relative to 10—100-nm roughness are important and that a synthesized electron-hole pair and SP model would be more appropriate.

With regard to the SP radiation, we have shown that the large amplitude roughness present on our electrochemically processed surface could be modeled by an autocorrelation function dominated by a single wave vector. Furthermore, this roughness produced the largest SP radiation and EARS signal, and corresponds well with values obtained by scanning electron micrographs.[14,17,21] Ritchie[26] has shown that the SP radiation spectrum is quite sensitive to the roughness autocorrelation functional form. Thus we propose the electron induced SP radiation mechanism as a simple means of comparing and evaluating the various roughened surfaces used in EARS studies. This method is well suited to UHV systems and allows an *in situ* determination of roughness properties.

ACKNOWLEDGMENTS

The author wishes to thank J. C. Buchholz, T. W. Capehart, and D. L. Simon for helpful discussions concerning the experiment and the interpretation given to this work. The author also thanks R. Teets for a critical reading of the manuscript.

---

[1]T. E. Furtak and J. Reyes, Surf. Sci. 93, 351 (1980).

[2]The acronym EARS is used here as an alternative to the ambiguous acronym SERS (surface-enhanced Raman scattering) which was originally coined in 1975 for stimulated electronic Raman scattering. See for example, D. Cotter *et al.*, Opt. Commun. 16, 256 (1976); J. Phys. B 9, 2165 (1976); IEEE J. Quantum. Electron. QE-14, 184 (1978); D. C. Hanna, M. Yuratich, and D. Cotter, *Nonlinear Optics of Free Atoms and Molecules,* Vol. 17 of the *Springer Series of Optical Science* (Springer, Berlin, 1979); Y. Takubo *et al.*, Appl. Phys. 24, 139 (1981).

[3]S. L. McCall, P. M. Platzman and P. A. Wolff, Phys. Lett. 77A, 381 (1980).

[4]J. C. Tsang, J. R. Kirtley, and T. N. Theis, Solid State Commun. 35, 667 (1980).
[5]M. Moskovits, Solid State Commun. 32, 59 (1979).
[6]M. Kerker, D. Wang, and H. Chew, Appl. Opt. 19, 4159 (1980).
[7]C. Y. Chen and E. Burstein, Phys. Rev. Lett. 45, 1287 (1980).
[8]D. A. Weitz, T. J. Gramila, A. Z. Genack, and J. I. Gersten, Phys. Rev. Lett. 45, 355 (1980).
[9]O. Hunderi and D. Beaglehole, Phys. Rev. B 2, 321 (1970).
[10]M. Kerker, O. Siiman, L. A. Bumm, and D. S. Wang, Appl. Opt. 19, 3253 (1980).
[11]J. A. Creighton, C. G. Blatchford, and M. G. Albrecht, J. Chem. Soc. Faraday Trans. 1 75, 790 (1979).
[12]M. E. Lippitsch, Chem. Phys. Lett. 74, 125 (1980).
[13]A. M. Glass, P. F. Liao, J. G. Bergman, and D. H. Olson, Opt. Lett. 5, 368 (1980).
[14]G. L. Eesley, Phys. Lett. 81A, 193 (1981).
[15]I. Pockrand and A. Otto, Solid State Commun. 35, 861 (1980).
[16]P. N. Sanda, J. M. Warlaumont, J. E. Demuth, J. C. Tsang, K. Christmann, and J. A. Bradley, Phys. Rev. Lett. 45, 1519 (1980).
[17]J. E. Rowe, C. V. Shank, D. Zwemer, and C. A. Murray, Phys. Rev. Lett. 44, 1770 (1980).
[18]C. A. Murray, D. L. Allara, and M. Rhinewine, Phys. Rev. Lett. 46, 57 (1981).
[19]S. S. Jha, J. R. Kirtley, and J. C. Tsang, Phys. Rev. B 22, 3973 (1980).
[20]J. R. Kirtley, S. S. Jha and J. C. Tsang, Solid State Commun. 35, 509 (1980).
[21]J. G. Bergman, D. S. Chemla, P. F. Liao, A. M. Glass, A. Pinczuk, R. M. Hart and D. H. Olson, Opt. Lett. 6, 33 (1981).
[22]W. H. Weber and G. W. Ford, Phys. Rev. Lett. 44, 1774 (1980).
[23]J. C. Tsang, J. R. Kirtley, and J. A. Bradley, Phys. Rev. Lett. 43, 772 (1979).
[24]G. L. Eesley, D. L. Simon, J. Vac. Sci. Technol. 18, 629 (1981).
[25]R. H. Ritchie, J. C. Ashley, and L. C. Emerson, Phys. Rev. 135, A759 (1964).
[26]R. H. Ritchie, Phys. Status Solidi 39, 297 (1970).
[27]R. E. Wilems and R. H. Ritchie, Phys. Rev. Lett. 19, 1325 (1967).
[28]M. S. Chung, T. A. Callcott, E. Kretschmann, and E. T. Arakawa, Surf. Sci. 91, 245 (1980).
[29]E. Kretschmann, T. A. Calcott, and E. T. Arakawa, Surf. Sci. 91, 237 (1980).
[30]C. Y. Chen, E. Burstein, and S. Lundquist, Proceedings of the U.S.-Japan Seminar on Inelastic Light Scattering [Solid State Commun. 32, (1979)].
[31]M. Udagawa, L. C. Chou, J. C. Hemminger, and S. Ushioda, Phys. Rev. B 23, 6843 (1981).
[32]E. Burstein, Y. J. Chen, C. Y. Chen, S. Lundquist, and E. Tossati, Solid State Commun. 29, 567 (1979).
[33]J. Billmann, G. Kovacs, and A. Otto, Surf. Sci. 92, 153 (1980).
[34]A. Otto, J. Timper, J. Billmann, and I. Pockrand, Phys. Rev. Lett. 45, 46 (1980).
[35]J. I. Gersten, J. Chem. Phys. 72, 5779 (1980).
[36]P. K. Aravind and H. Metiu, Chem. Phys. Lett. 74, 301 (1980).
[37]R. Naaman, S. J. Buelow, O. Cheshnovsky, and D. R. Herschbach, J. Phys. Chem. 84, 2692 (1980).